JCHS

TU Delft OPEN Publishing

JOURNAL OF COASTAL AND HYDRAULIC STRUCTURES

Vol. 6, 2026, 52

Quantification of Salt Intrusion Caused by Navigation Locks and Their Operation for Policy Analysis, Water Management or Salt Dispersion Modelling

Otto M. Weiler [1], Tjerk Vreeken [1], Sam D. Maijvis [1], Nino L. Zuiderwijk [1], and Tom S. D. O'Mahoney [1 *]

Abstract

Sea locks can be a source of saltwater intrusion into inland surface waters, coastal reservoirs or canals. Typical analytical models for calculating the amount of salt intrusion are either calibrated on existing locks or make conservative assumptions about the operation (for instance, assuming full exchange of the lock chamber contents upon opening the gate). This paper presents a model which can quantify the salt intrusion based on building blocks describing the volume exchanges in the different lock phases. The model can be used stand-alone or in combination with salt dispersion modelling to determine the requirements for lock operation, in the evaluation of mitigating measures, or in the design of new locks within the context of water management of the inland water system. Validation using field measurements showed a model underestimation of 7–10%. This model can be readily applied to future unknown situations, such as increased ship traffic, rising sea levels and/or changes in lock operation. In addition, the application of mitigation measures, such as bubble screens, can be included. The relative effect of these inputs is illustrated here using generic examples. It is shown that lock operation has a significant effect on the salt intrusion through the lock and that under climate change inland freshwater systems, for which sea locks are the primary or dominant source of salt intrusion, may be threatened more seriously by drought (reduced flushing discharge) than by sea level rise.

Keywords

Sea lock, navigation lock, salt intrusion, water management, event-based model, box model

[1] Deltares, Delft, The Netherlands
* tom.omahoney@deltares.nl

Research Article. **Submitted:** 17 July 2025. **Reviewed:** 23 September 2025. **Accepted** after double-anonymous review: 17 February 2026. **Published:** 11 March 2026.

DOI: 10.59490/jchs.2026.0052.

Cite as: Weiler, Otto M.; Vreeken, Tjerk; Maijvis, Sam D.; Zuiderwijk, Nino L.; O'Mahoney, Tom S. D. (2026): Quantification of Salt Intrusion Caused by Navigation Locks and Their Operation for Policy Analysis, Water Management or Salt Dispersion Modelling, Journal of Coastal and Hydraulic Structures, 6, https://doi.org/10.59490/jchs.2026.0052

ISSN: 2667-047X online

1 Introduction

Saltwater intrusion threatens freshwater resources in many delta areas worldwide (IPCC, 2014). Intrusion can occur into the coastal groundwater aquifers (Werner et al., 2012), into open estuaries (MacCready and Geyer, 2010; Savenije, 2012) and into inland freshwater lakes, canals and waterways (PIANC, 2021). Among the drivers of saltwater intrusion are those related to climate change, sea level rise (Werner and Simmons, 2009) and drought severity and frequency

(Mosley, 2015; Galván et al., 2016; Hendriks et al., 2014), but also human driven direct changes in the delta (such as channel deepening (Ralston and Geyer, 2019; van Rijn et al., 2018); freshwater extraction (Bain et al., 2019; El-Agha et al., 2020), or dams (Prasad et al., 2018)). Now, many researchers are studying the effects of climate change on saltwater intrusion in delta areas (Robins et al., 2016; Ferguson and Gleeson, 2012). Efforts have been made to quantify the effect of sea level rise on groundwater (Werner and Simmons, 2009; Ferguson and Gleeson, 2012; Oude Essink et al., 2010). For studies in surface waters, models at different scales and dimensions are utilised: from analytical models (Nguyen and Savenije, 2006; Savenije, 2012); 1D branching models (Vu et al., 2018); 2D branching models (Wang, 1983); to fully 3D hydrodynamic models (Akter et al., 2019; Bricheno et al., 2021; Chen et al., 2016). In estuaries there are examples from the UK (Lowe et al., 2009), the US (Hagen et al., 2013), Mekong delta (Vu et al., 2018; Nguyen and Savenije, 2006), Brahmaputra Delta (Akter et al., 2019; Bricheno et al., 2021), and in Spain (Galván et al., 2016). The effects of drought have also been looked at (Mosley, 2015; Hendriks et al., 2014; Galván et al., 2016; Gong et al., 2013).

In the Netherlands, a country with a high population density in a low-lying delta, salt intrusion can occur via groundwater, open estuaries and into freshwater lakes and canals. In these lakes (IJsselmeer, Volkerak-Zoommeer) protected from the sea by large dams, or in canals (North Sea Canal) saltwater intrusion is often dominated by intrusion through shipping locks in the enclosure dams (Genseberger and Bijlsma, 2016). In general, salt concentrations are kept below relevant criteria by flushing the canal or lake with freshwater taken from rivers and with drainage water from polders. Due to climate change, periods of low rainfall and low river discharge are increasing in duration and intensity, leading to limitations in the availability of freshwater for flushing and thus to rising salt concentrations. A second threat to the salt concentrations is the construction of newer and bigger navigation locks. Examples in the Netherlands include projects in IJmuiden (Nogueira et al., 2018) and Terneuzen (Martens et al., 2018). Other examples of freshwater lakes and canals where the shipping locks form the primary source of salt intrusion are the Panama Canal (Parchure et al., 2000; Jongeling, 2003) and the Washington Ship Canal (Rinehimer et al., 2019).

Hydrodynamic models of these systems require a boundary condition for the salt flux across the shipping locks (Genseberger et al., 2021) because they are either incapable of capturing the necessary non-hydrostatic flow phenomena around the locks or because others methods, such as Computational Fluid Dynamics (CFD) models, are too computationally expensive to be run for realistic variations in conditions and lock operations. This paper details a calculation method, a set of formulae, that is capable of quantifying the salt intrusion at sea locks, taking into account the geometry, the boundary conditions (water levels and salt concentration at both lock heads), the lock operation and mitigating measures. This set of formulae, called here simply the Sea Lock Formulation (SLF) can be applied at varying levels: from high level policy analysis type studies, to short-term forecasts for water management and providing boundary conditions for detailed 3D dispersion modelling. The source code of the SLF is available on GitHub as *D-SLF* and the model is published as Python package *pyzsf* (from the Dutch word 'Zeesluisformulering', abbreviated as ZSF).

Specifically for the Netherlands, models have been developed for a variety of purposes. There are 1D (Prinsen et al., 2015; Van den Brink et al., 2019), 2D (Haasnoot et al., 2020) and 3D models of the Rhine delta in the Netherlands that have mostly been used to study salt intrusion into the open part of the estuary via the Rotterdam Waterway (van Rijn et al., 2018) during times of drought. These surface water models often use the D-HYDRO suite of packages, which is Open Source and also applied to many other locations worldwide (Akter et al., 2019; Galván et al., 2016; Martyr-Koller et al., 2017). The development of these packages is described in a recent review (De Goede, 2020). Another example is a 2D model such as MIKE 21 FM (Wang et al., 2024).

The response of policymakers to all the quantification studies of salt intrusion is also of great importance (Hagen and Irish, 2013). When doing policy analysis for different scenarios also *mitigation* measures can be studied if the model includes accurate estimates of their effectiveness. For groundwater, some mitigation measures have been studied (Costall et al., 2020; Huizer et al., 2017) but for estuaries there are very few options available. Possible measures include the redirection of river discharge by means of existing weirs and discharge sluices and other operational water management actions (Ferguson and Gleeson, 2012; Ekin Aydin et al., 2019; Augustijn et al., 2011) or the creation of temporary sills (McAnally and Pritchard, 1997; Cuthbertson et al., 2018).

For salt intrusion through navigation locks at the interface between the sea and lakes or canals many mitigation measures are available. The physical processes are well known and have been studied extensively. The primary process is the lock exchange flow driven by the difference in density of water inside and outside of the lock chamber (Brooke Benjamin, 1968; Shin et al., 2004). Summaries of the different lock-levelling systems with integrated salt water mitigation

systems are described in Van der Kuur (1985) and Kerstma et al. (1994). The effectiveness of bubblescreens in reducing the lock-exchange flows when the lock gates are opened has been well studied (Abraham and van den Burgh, 1964; Keetels et al., 2011; Uittenbogaard et al., 2015). The more recent work of Keetels et al. also provides empirical relations for the effectiveness of larger lock sills and 'waterscreens' in reducing the lock-exchange flows. The effectiveness of flushing salt water around or through the lock-chamber during various phases of the locking cycle are also available (Mausshardt and Singleton, 1995; Keetels et al., 2011; Kerstma et al., 1994).

These studies provide valuable information on the effectiveness of these mitigation measures within a particular phase of the locking cycle. The net effect on the salt intrusion after all processes of the locking cycle have been performed (levelling, lock exchange and ship displacement from ships exiting and entering) requires information on the lock operation. Details of this operation have a larger influence than is often assumed. Where these studies provide quantification of the effectiveness over the entire locking-cycle it is implicitly assuming that the lock operation doesn't change from that studied. However, the density of ship traffic has a large effect on the amount of salt intrusion, regardless of other water management choices, as it largely determines the gate-open times and the amount of ships per locking cycle and consequently the net effectiveness of the measures. For instance, a bubble screen can only be effective if the gate-open times are kept short and if they *are* kept short the salt intrusion is also reduced in the subsequent locking cycle as the lock chamber remains brackish, reducing the density difference and consequently the exchange flows in the following locking phases.

Some studies (Augustijn et al., 2011; Parchure et al., 2000; Jongeling, 2003; Rinehimer et al., 2019) try to account for the total effect of the lock operations on the net transport by means of a so-called exchange coefficient which was first introduced by Kerstma et al. (1994). This coefficient calibrates the net salt intrusion of the lock to measurements or assumptions about the lock operations (often conservatively assuming full exchange of the lock chamber during the gate open phase or that the gate-open times will not change). As such this method is not able to predict changes in the lock operation owing to changes in the system, such as new ways of operation, increased shipping traffic, new locks or changing hydrological conditions. A model based on the underlying processes of the lockage operation per phase would be able to quantify these effects. Some models along these lines have been developed previously ('Zoutlekmodel' (Uittenbogaard, 2010) and 'WANDA-Locks' (Van der Ven et al., 2015; De Groot, 2015)) and applied (Van der Ven et al., 2018; Weiler et al., 2015) but these are not freely available or supported at present and remain unpublished in the scientific literature, being only available as technical reports in Dutch. The approach presented in the current paper is similar in principle to these earlier models and makes use of some of the empirical relations developed in the studies named above.

Incorporating the salt intrusion per phase of the locking cycle also has other advantages. It allows for a more accurate (in time) definition of boundary conditions as used in numerical models for the dispersion of salt water from the navigation locks towards the relevant locations at the freshwater intakes for agriculture or drinking water, et cetera. In addition, a method for the quantification of exchanges per phase is important as it brings an understanding of the parameters (and phases) that drive the salt intrusion, which can be used to design effective mitigation measures. When the method takes all influences into account, only then can it serve to support decisions taken in day-by-day water management and lock operation aimed at controlling salt concentrations at key locations.

The presented event-based box model is compact and computationally efficient and thereby suitable to be included in hydrodynamic software (such as D-HYDRO suite (De Goede, 2020)) as used for the modelling of salt dispersion in lakes and canals. The computational approach allows for the use of large time steps in the numerical model for salt dispersion, so that this model can cover a large area and a large period of time at limited computational effort. This implies the requirement to make reliable computations without accurately describing each individual locking cycle. Instead, aggregated data on the lock operation suffice as input. This feature is also very helpful when making forecasts, such as in water management: details of the locking operation are relevant but are not always known ahead of time. Furthermore, the method includes the effects of measures aimed at limiting salt intrusion, such as the application of bubble screens or sills. It is also possible to use a flushing flow through the lock chamber in the SLF (Van Beek, 2021), but this option will not be described further in this paper. Development of the SLF is ongoing and will add additional mitigation measures and coupling with network models of the surrounding water system such that mitigation measures taken in the wider system can also be evaluated.

Overall, the SLF can be characterised as a method which does not necessarily exactly reproduce the hydrodynamic phenomena as related to each separate lockage cycle, but it does provide a proper quantification of the salt intrusion on average over time. The present paper describes the methodology, validation and applications of the SLF.

2 Methodology

The chosen approach for the quantification of the salt intrusion through shipping locks is to set up the equations of flows in and out of the lock for all phases of the locking cycle separately. A locking cycle basically consists of four phases: levelling to the fresh side, lock exchange to the fresh side, levelling to the salt side and lock exchange to the salt side. The result is an event-based box model in which the volumes of water exchanged due to levelling, the lock exchange process when opening the gates and the displacement by ships are calculated, along with a salt concentration for each volume, and these are added together to find the total volumes and their salt contents that go in and out of the lock at both lock heads. The model then predicts salt mass fluxes based on volume balances multiplied by the lock chamber-averaged salt concentrations. Note that this phase-wise approach is not the same as a fixed time-step approach (meaning a specified Δt, as is the case in many transient models) as the computation is performed per phase of the lockage cycle, which is a discrete event that does not have a fixed duration. The method can also be used to calculate the cycle-averaged flows of water into and out of the lock chamber at both lock heads, each with a corresponding salt concentration. The flows going into the lock have the salt concentration as prescribed by the boundary condition, which may come from measurements or from another hydrodynamic model of dispersion in the adjacent water bodies. The flows coming out of the lock will have a salt concentration as calculated by the method.

When detailed data on the individual cycles is available, for instance through registrations on the lock under study, a calculation of the phase-by-phase transport is possible (referred to as the phase-wise SLF). When no registrations are available, the lockage cycle is parameterised based on some average values of the lock operation i.e. how long the gate is open and how much time is required for levelling (referred to as the cycle-averaged SLF). These parameters are then translated into a repeating pattern of locking phases. The cycle-averaged values of discharges and salinities are obtained through iteration.

In going through the consecutive phases of the cycle, the method assumes ‘instant’ mixing of the water inside the lock chamber every time water has entered the lock chamber. In this way it finds a new value for the salt concentration in the lock chamber that can be used to calculate the next phase. Updating the salt concentration in the lock after each phase is important as this determines the salt concentration of the water leaving the lock, but also provides an input to the calculation of the lock exchange when one of the lock gates opens.

2.1 Conventions and assumptions

2.1.1 Flow direction

In the formulae presented in this paper the positive direction of flow is from the freshwater side, the canal or river, into the lock chamber and from the lock chamber towards the sea. When the canal has a higher water level than the sea, all levelling flows will have a positive sign. Lock exchange flows travel both ways, and therefore will have a positive and a negative sign. The salt is transported with the water, and hence a net salt intrusion to the freshwater side, expressed in a dry load, will have a negative sign.

2.1.2 Vertically mixed

As a consequence of the lock exchange flows there will often be stratification both in the approach harbours and in the lock chamber. However, the method presented uses depth averaged salt concentration values only. This also implies that after each phase in the lockage cycle, instant and complete mixing of the water in the lock chamber is assumed, leading to a new depth averaged value for the next phase.

2.1.3 Boundary conditions

The boundary conditions on either side of the lock, the fresh side and the salt side, consist of a water level with a corresponding salt concentration S [kg/m^3] or density ρ [kg/m^3]. The salt concentration here is consistently used as the kilograms of salt in a cubic metre of water. Conversion to salinity (in PSU or ppt) or even to chloride concentration should be done carefully, if necessary, for comparison with other studies. In the present study we maintain this simplified definition of salt concentration as it is designed as a practical engineering tool and the requirements for the level of accuracy in salt concentration is not high, as is suggested by the assumption of vertical mixing. The water levels (h) on each side of the lock are defined as h_F for the water level on the fresh side, and h_S for the water level on the salt side. These water levels are expressed relative to a vertical chart datum [mDAT].

2.1.4 Phases of the lockage cycle

The phases of the lockage cycle are shown in Figure 1, for two situations. The left-hand column shows the phases for a situation where the water level at sea is lower than on the freshwater side ($h_S < h_F$). This situation is indicated with 'LT' (as in low tide). The righthand column covers the situation where the water level at sea is higher than at the freshwater side ($h_S \geq h_F$), indicated with 'HT'. The lock is levelled to either the freshwater or saltwater side in phases 1 and 3, respectively. Phases 2 and 4, in which the gates are open on respectively the freshwater or the saltwater side, are divided into three subphases: ships exiting the lock chamber (a), lock exchange flow (b), and ships entering the lock chamber (c). This division is detailed further in Section 2.3.2. It is important to note that in case of multiple ships, the total displacement of the ships is treated as if it was a single ship.

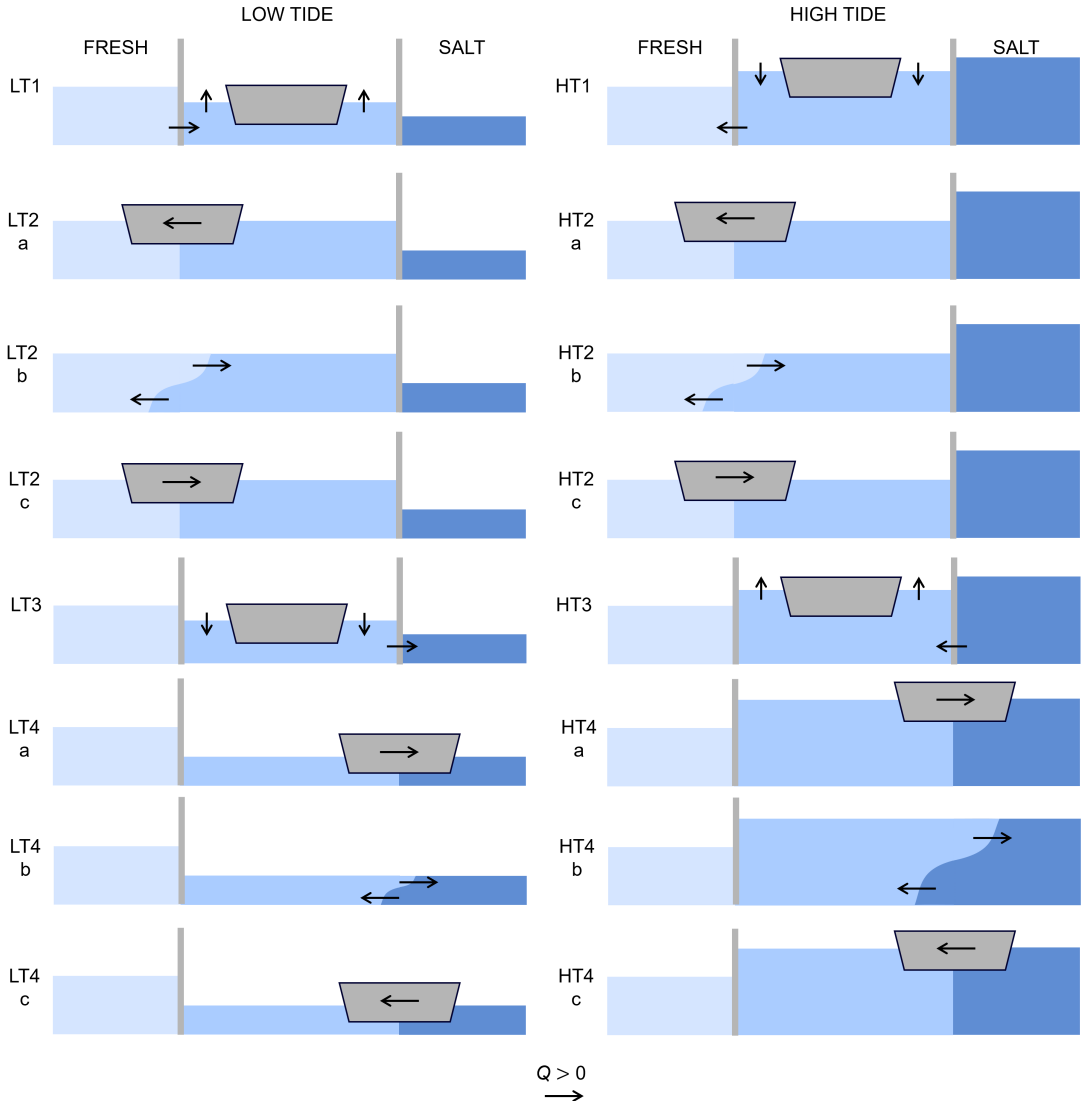

Figure 1: The schematization into (sub)phases of a lockage cycle during low (left) and high tide (right) in the SLF.

The dominant flow direction of rivers and deltas was chosen as the positive direction of flows in the SLF, meaning downstream, towards the sea, from fresh to salt. This sign convention (see Section 2.1.1), is shown in Figure 1 for the discharge Q [m^3/s]: positive in the downstream direction, meaning towards the sea. This same convention holds for transported volumes V [m^3] and transported salt mass M [kg]. Due to this sign convention, salt intrusion is the transport of salt in the negative direction.

2.1.5 Lock geometry

The water level in the lock is given as h_L [mDAT]. The lock has a length L_L [m], a width W_L [m], and the lock bottom is located at z_L [mDAT]. The formulae below are limited to a geometry with a constant bottom level: in both approach harbours, in both lock heads and in the lock chamber. The water depth H [m] at the active lock head is then given by:

$$H_F = h_F - z_L \tag{1}$$

$$H_S = h_S - z_L \tag{2}$$

The volume of water in the lock chamber [m^3] when the lock is levelled with the fresh side and salt side respectively are:

$$V_{L,F} = L_L W_L H_F \tag{3}$$

$$V_{L,S} = L_L W_L H_S \tag{4}$$

2.2 Processes in the lock-cycle

To set up the equations, it is necessary to define the various physical quantities. An understanding of these physical quantities should be based on an understanding of the relevant processes (levelling, lock exchange and ship displacement). Therefore, we first (briefly) introduce these processes, followed by explaining the quantities that will appear in the equations later. All variables are consistently labelled with suffixes L, F and S, which refer to the lock chamber, freshwater side and saltwater side, respectively.

2.2.1 Levelling

The locking of ships is in essence about overcoming a difference in water level. By letting a ship moor temporarily in a lock chamber, and by changing the water level in this lock chamber, the water level difference can be bridged. This process is called levelling[(1)]. Raising the water level is done by letting water in from the high side ('filling') and lowering the water level is done by letting out water to the low side ('emptying').

In a LT-type situation a volume of freshwater $V_{Lev,LT}$ will be added to the lock chamber in phase LT1 and leave the lock chamber in phase LT3. This volume, moving from the freshwater side towards the saltwater side, is defined as the LT levelling volume. In a HT-type situation, the levelling volume $V_{Lev,HT}$ moves in the other direction. This volume is defined as the HT levelling volume. Depending on the difference in water level at both sides of the lock, one of the two will be equal to zero:

$$\text{LT: } V_{Lev,LT} = L_L W_L (h_F - h_S), \quad V_{Lev,HT} = 0 \tag{5}$$

$$\text{HT: } V_{Lev,LT} = 0, \quad V_{Lev,HT} = L_L W_L (h_S - h_F) \tag{6}$$

(1) In practice, lock gates are often opened while there is still a small head difference. The magnitude of this remaining head difference depends on density differences and levelling system geometry (Nogueira et al., 2023; PIANC, 2021), and is levelled out while the doors are opened. In the SLF, the salt transport during levelling includes the complete levelling volume. Thereby the next phase starts with water levels being equal inside and outside of the lock.

2.2.2 Lock Exchange

Where there is a difference in salt concentration - and with that a difference in density - between both sides of the lock and therefore between the lock chamber and its inner and outer approach harbour, a current will start to develop when the gates on either end are opened. This current is called a density current, and the phenomenon of this current exchanging the saltwater in the lock chamber with freshwater (or vice versa) is called 'lock exchange'. The less dense freshwater will start to float on top of the denser saltwater and move to the salt side. After reflection of the density current on the closed gates, the process continues until just about the entire lock volume has been exchanged or until the gates are closed.

The lock exchange is often the most important process for salt intrusion through shipping locks. This is simply because the depth of the lock chamber is often larger than the lockage prism. The role of ships in this process is elaborated upon in Section 2.2.3 but the salt intrusion owing to ship displacement is small compared to the lock exchange as ship volume is relatively small compared to the lock volume in most cases. The process of lock exchange in time can be approximated with a hyperbolic tangent function (Abraham and van den Burgh, 1964). The exchanged volume V_U is then expressed as:

$$V_U = V_L \tanh\left(\frac{\eta T_{open}}{T_{LE}}\right) \tag{7}$$

where T_{open} is the gate-open time, the period during which the gate is open after levelling, V_L is the lock volume, and T_{LE} is the (theoretical) time it takes for the density current to travel the length of the lock chamber twice, to the closed gate and back to the active open gate after reflection. This assumes a constant velocity of the density current consistent with the theoretical value of Brooke Benjamin (1968). This velocity, c_i, is determined by the relative density difference $\Delta\rho/\bar{\rho}$, the gravitational acceleration g, and the water depth H, in the respective active lockhead. Therefore

$$T_{LE} = \frac{2L_L}{c_i} = \frac{2L_L}{\frac{1}{2}\sqrt{\frac{gH\Delta\rho}{\bar{\rho}}}} \tag{8}$$

Equation (7) also includes bubble screen efficiency η, which effectively slows down the lock exchange. This parameter will be further elaborated upon in Section 4.1. Figure 2 shows the relative lock exchange (V_U/V_L) as a function of the relative gate-open time (T_{open}/T_{LE}). The blue solid line in Figure 2 shows that the lock chamber will fully exchange ($V_U/V_L \to 1$) if the lock gates are open for a long time.

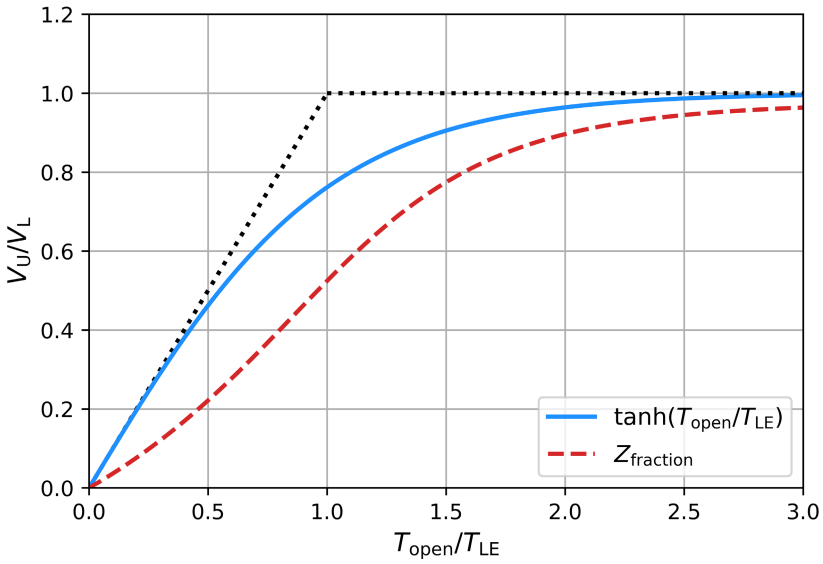

Figure 2: The relative lock exchange V_U/V_L as a function of the relative gate-open time T_{open}/T_{LE}. The black dotted line represents the theoretical lock exchange. The SLF calculates the exchanged volume using a hyperbolic tangent (solid blue). Consecutive partial lock exchanges slow down the total resulting exchange, resulting in the parameter $Z_{fraction}$ (dashed red, see Equation (9)).

If the lock chamber does not exchange fully, the following lock exchange will be slower because the difference in salt concentration between lock chamber and approach harbour has become smaller. For the same gate-open time, this results in less exchange and therefore a smaller transported salt mass M. This mechanism can be described using the dimensionless parameter Z_{fraction} (red dashed line in Figure 2):

$$Z_{\text{fraction}} = \frac{\bar{M}}{\bar{V}_{\text{L}}(S_{\text{S}} - S_{\text{F}})} = \frac{\frac{1}{2}(M_{\text{F}} + M_{\text{S}})}{\frac{1}{2}(V_{\text{L,F}} + V_{\text{L,S}})(S_{\text{S}} - S_{\text{F}})} \tag{9}$$

This parameter describes the salt transport per cycle, expressed as a fraction of the salt transport that would occur during a complete lock exchange at both lock heads (the lock chamber volume times the salt concentration difference between both sides of the lock chamber). The red curve lies significantly lower than the blue curve in Figure 2, showing the self-reinforcing effect of consecutive partial lock exchanges. This shows that the achievable reduction of salt transport by reducing the gate-open times can be much greater when looking at a sequence as opposed to a single lock exchange.

2.2.3 Ship displacement

The presence of ships in the locking cycle influences the lock exchange in two ways:

1. When a ship enters a lock chamber, water is pushed out of the lock chamber. The amount of water that leaves the lock is equal to the water displacement of the ship. Conversely, when ships exit the lock chamber, water will flow from the approach harbour into the lock chamber to fill the 'hole' left by the ships.
2. The upwards levelling of a lock chamber means that water comes in from the high side. In case of a lock between salt- and freshwater, it is likely that the water that enters has a different salt concentration than the water inside the lock chamber. At the end of levelling the lock chamber will therefore have a new average salt concentration. When determining this average salt concentration, we need to take into account that, when ships are present in the lock, there is less water inside the lock chamber.

In case of a complete lock exchange, the volume of the ship in the lock reduces the amount of water in the lock, and thereby the total amount of salt that can be transported. In case of a partial lock exchange, for instance in the case of bubble screens, the movement of ships in and out of the lock increases the exchange of water between the lock chamber and the approach harbour on either side. This leads to an increase in salt intrusion. The presence of ships inside the lock chamber does not have influence on the amount of water that is needed for levelling.

In the formulation of transports through the lock it is not about the individual but about the total water displacement of the ships per cycle. Note that the upstream and downstream displacement do not have to be equal. For example, when through a certain lock more cargo is imported than exported, this will be represented accordingly in the water displacements in both directions. With that, also a net discharge through the lock can arise.

2.3 Equations per lockage phase

In this section the formulae describing each phase are presented. The formulae have been simplified by expressing the salt concentration in [kg/m^3], allowing easy relations between the volume of water [m^3] and mass of salt [kg]. The density is then calculated from salt concentration and temperature using the UNESCO-formulation (UNESCO, 1981), under the assumption that the expression of salt concentration in [kg/m^3] and salinity in [PSU] are equivalent (see Section 2.1.3).

2.3.1 Phase 1: Levelling towards the freshwater side

Using the levelling volumes as defined in Equations (5) and (6), the transported salt mass due to levelling can be described as:

$$\text{LT: } M_{\text{F,LT1}} = V_{\text{Lev,LT}} S_{\text{F}} \tag{10}$$

$$\text{HT: } M_{\text{F,HT1}} = -V_{\text{Lev,HT}} S_{\text{L,S}} \tag{11}$$

These two formulae can be combined into one, as either of the two volumes will be zero.

$$M_{\mathrm{F},1} = V_{\mathrm{Lev,LT}} S_{\mathrm{F}} - V_{\mathrm{Lev,HT}} S_{\mathrm{L,S}} \tag{12}$$

After this phase, the salt concentration in the lock chamber has changed (to $S_{\mathrm{L,S,Lev}}$), depending on the level difference. In a LT-type situation the salt concentration in the lock chamber will reduce due to mixing with added freshwater. In a HT-type situation water will flow from the lock and the salt concentration in the lock chamber will not change.

$$\mathrm{LT}: S_{\mathrm{L,S,Lev}} = \frac{(V_{\mathrm{L,S}} - V_{\mathrm{Ship,Up}}) S_{\mathrm{L,S}} + V_{\mathrm{Lev,LT}} S_{\mathrm{F}}}{V_{\mathrm{L,F}} - V_{\mathrm{Ship,Up}}} \tag{13}$$

$$\mathrm{HT}: S_{\mathrm{L,S,Lev}} = S_{\mathrm{L,S}} \tag{14}$$

This salt concentration is subsequently used as the initial salt concentration in the lock for the next phase.

2.3.2 Phase 2: Lock exchange at the freshwater side

While the gates are open on one side there are various processes that take place that contribute to the transport of salt over the opened lock head. These processes are:

a) Salt transport due to ships exiting the lock chamber

b) Salt transport due to the lock exchange flow

c) Salt transport due to ships entering the lock chamber

If the transports due to these processes are independently calculated before adding them up, there is a possibility of the salt transport being too high. This would result in a salt concentration in the lock chamber that is lower than the fresh side, or higher than the salt side. To prevent this from happening, Phase 2 has been divided into three subphases, corresponding to the list above. Each of these subphases leads to a new intermediate salt concentration of the lock chamber.

The salt transport due to ships exiting the lock, and the subsequent salt concentration in the lock afterwards, is given by:

$$M_{\mathrm{F,2a}} = V_{\mathrm{Ship,Up}} S_{\mathrm{F}} \tag{15}$$

$$\mathrm{LT}: S_{\mathrm{L,2a}} = \frac{S_{\mathrm{L,S,Lev}} (V_{\mathrm{L,F}} - V_{\mathrm{Ship,Up}}) + M_{\mathrm{F,2a}}}{V_{\mathrm{L,F}}} \tag{16}$$

Lock exchange starts as soon as the gates open. The lock exchange manifests itself as two opposing currents: the freshwater has a lower density and starts to float on top of the heavier saltwater, which sinks below the freshwater. As a consequence, an upper layer of freshwater starts to move towards the saltwater side, and a lower layer of saltwater starts to move towards the freshwater side. The mass of salt that is transported in this phase is determined by the exchanged volume and the salinities in the lock chamber and the approach harbour.

$$M_{\mathrm{F,2b,LE}} = V_{\mathrm{U,F}} S_{\mathrm{F}} - V_{\mathrm{U,F}} S_{\mathrm{L,2a}} \tag{17}$$

After this phase of lock exchange, a new salt concentration in the lock will have established:

$$S_{\mathrm{L,2b}} = \frac{S_{\mathrm{L,2a}} V_{\mathrm{L,F}} + M_{\mathrm{F,2b,LE}}}{V_{\mathrm{L,F}}} \tag{18}$$

The salt transport due to ships entering the lock is given by:

$$M_{\mathrm{F,2c}} = -V_{\mathrm{Ship,Down}} S_{\mathrm{L,2b}} \tag{19}$$

The salt concentration of the lock does not change when a ship enters the lock (assuming a fully mixed lock chamber before entry). In total for phase 2 the transported salt mass and the salt concentration afterwards are given by:

$$M_{\mathrm{F,2}} = M_{\mathrm{F,2a}} + M_{\mathrm{F,2b,LE}} + M_{\mathrm{F,2c}} \tag{20}$$

$$S_{\mathrm{L,2}} = \frac{S_{\mathrm{L,S,Lev}}(V_{\mathrm{L,F}} - V_{\mathrm{Ship,Up}}) + M_{\mathrm{F,2}}}{(V_{\mathrm{L,F}} - V_{\mathrm{Ship,Down}})} \tag{21}$$

2.3.3 Phase 3: Levelling to the saltwater side

Just like in Phase LT1 and HT1 it holds that either $V_{\mathrm{Lev,LT}}$ or $V_{\mathrm{Lev,HT}}$ is zero by definition. The equations for both tidal phases can therefore be summed up into a single equation:

$$M_{\mathrm{S,3}} = V_{\mathrm{Lev,LT}} S_{\mathrm{L,F}} - V_{\mathrm{Lev,HT}} S_{\mathrm{S}} \tag{22}$$

In the situation around low tide, water is extracted from the lock chamber to lower the level, which does not change the salt concentration in the lock chamber. When levelling at high tide, the average salt concentration of the water in the lock chamber rises because saltwater is let in. To calculate this new salt concentration, the water displacement by ships present in the lock chamber has to be taken into account. Consequently, the salt concentration in the lock after this phase is given as:

$$\mathrm{LT}: S_{\mathrm{L,F,Lev}} = S_{\mathrm{L,F}} \tag{23}$$

$$\mathrm{HT}: S_{\mathrm{L,F,Lev}} = \frac{(V_{\mathrm{L,F}} - V_{\mathrm{Ship,Down}})S_{\mathrm{L,F}} + V_{\mathrm{Lev,HT}} S_{\mathrm{S}}}{V_{\mathrm{L,S}} - V_{\mathrm{Ship,Down}}} \tag{24}$$

2.3.4 Phase 4: Lock exchange at the saltwater side

Phase 4 (just like Phase 2) has been divided into three subphases, corresponding to the list above. Each of these subphases leads to a new intermediate salt concentration of the lock chamber:

The salt transport due to ships exiting the lock, and the subsequent salt concentration in the lock afterwards, is given by:

$$M_{\mathrm{S,4a}} = -V_{\mathrm{Ship,Down}} S_{\mathrm{S}} \tag{25}$$

The mass of salt that is transported in the lock-exchange sub-phase is determined by the exchanged volume and the salinities in the lock chamber and the approach harbour.

$$M_{\mathrm{S,4b,LE}} = V_{\mathrm{U,S}} S_{\mathrm{L,4a}} - V_{\mathrm{U,S}} S_{\mathrm{S}} \tag{26}$$

The salt transport due to ships entering the lock is given by:

$$M_{\mathrm{S,4c}} = V_{\mathrm{Ship,Up}} S_{\mathrm{L,4b}} \tag{27}$$

In total for phase 2 the salt transport and the salt concentration afterwards are given by:

$$M_{\mathrm{S,4}} = M_{\mathrm{S,4a}} + M_{\mathrm{S,4b,LE}} + M_{\mathrm{S,4c}} \tag{28}$$

$$S_{\mathrm{L,4}} = \frac{S_{\mathrm{L,F,Lev}}(V_{\mathrm{L,S}} - V_{\mathrm{Ship,Down}}) + M_{\mathrm{S,4}}}{(V_{\mathrm{L,S}} - V_{\mathrm{Ship,Up}})} \tag{29}$$

2.4 Cycle-averaged equations

For instances that a detailed time series of gates and valve operations are not available, or a detailed times series of the corresponding fluxes is not necessary, average values for these parameters can be used. The description of the lock operation on an aggregated level starts with the number of cycles per day. Additionally, there must be information on the duration of levelling (potentially as a function of the water level on the sea side, varying with the tide) and information on the time required for opening and closing lock gates. From these data one can derive the average time that lock gates are open in each lock head: the time available for lock exchange (gate-open times).

Based on the volumes per locking cycle we now can, for each of the lock heads, determine the total transported volumes with their corresponding salinities. From these volumes the cycle-averaged flows can be determined. In a calculation based on these aggregated data, the lockage cycle is run through a number of times, taking into account constant hydraulic boundary conditions. The constant (or average) boundary conditions should be chosen such that they are representative for the period of time in which the user is interested, for example a yearly average or a period of drought. After some iterations the transported volumes and their salinities per phase have reached an equilibrium that is independent of the initial salt concentration in the lock chamber and are therefore representative for the salt fluxes which would be achieved on average. This same procedure can be repeated with varying input variables (under tides and varying salt concentrations) to calculate how average salt fluxes vary under these varying conditions.

2.4.1 Fresh side

The combined equation for the fresh side gives the total transport of the entire locking cycle. This equation is as follows:

$$M_{\mathrm{F}} = M_{\mathrm{F,1}} + M_{\mathrm{F,2}} \tag{30}$$

The cycle-average mass flux is then given as $\dot{M}_{\mathrm{F}} = M_{\mathrm{F}}/T_{\mathrm{Cycle}}$. The volumes that are discharged towards the fresh side (lock to lake) and vice versa (lake to lock) are respectively:

$$V_{\text{lock to lake}} = V_{\mathrm{Lev,HT}} + V_{\mathrm{U,F}} + V_{\mathrm{Ship,Down}} \tag{31}$$

$$V_{\text{lake to lock}} = V_{\mathrm{Lev,LT}} + V_{\mathrm{U,F}} + V_{\mathrm{Ship,Up}} \tag{32}$$

The discharge and salt concentration which is transported onto the lake is therefore as follows:

$$Q_{\text{lock to lake}} = \frac{V_{\text{lock to lake}}}{T_{\text{cycle}}} \tag{33}$$

$$S_{\text{lock to lake}} = \frac{(M_{\mathrm{F}} - V_{\text{lake to lock}} S_{\mathrm{F}})}{V_{\text{lock to lake}}} \tag{34}$$

2.4.2 Salt side

The combined equation for the salt side gives the total transport of the entire locking cycle. This equation is as follows:

$$M_{\mathrm{S}} = M_{\mathrm{S,3}} + M_{\mathrm{S,4}} \tag{35}$$

The cycle-average mass flux is then given as $\dot{M}_{\mathrm{S}} = M_{\mathrm{S}}/T_{\mathrm{Cycle}}$. In addition to the mass fluxes, the discharges and salinities going in and out of the sea lock on both sides are also computed.

2.4.3 Calibration of cycle-averaged approach to an irregular lockage pattern

Averaged over time, the fluxes of water and salt as calculated in the cycle-averaged approach should be the same as the values calculated in the phase-by-phase approach. In reality, this will usually not be the case: spreading the average number of lockage cycles per day evenly over 24 hours will result in a larger value for the salt intrusion than when considering a realistic irregular pattern of lockages. This has to do with the duration that the lock gates are open and the

lock exchange flow that takes place. Spreading the available time evenly over all instances of lock gates being open maximises the transport of salt towards the canal or lake. Irregular lockages will lead to less salt intrusion; a shorter gate-open time causes a relatively large reduction of salt intrusion, whereas a longer gate-open time will cause a relatively small increase as the maximum lock exchange is limited to the volume of the lock chamber.

In order to take this into account, a calibration parameter is introduced to reduce the *average* gate-open time to a *representative* gate-open time, by which the cycle-averaged fluxes and salt intrusion can be adjusted to the average of a phase-by-phase computation. This calibration parameter c_{DOT} ranges between 0 and 1, where $c_{\mathrm{DOT}} = 1$ is conservative, meaning no variation over the day. If, for example, the locking frequency is smaller during the night than during the day, $c_{\mathrm{DOT}} < 1$. Altogether this results in the *representative* gate-open time T_{open}:

$$T_{\mathrm{open}} = c_{\mathrm{DOT}} T_{\mathrm{open,avg}} \tag{36}$$

where $T_{\mathrm{open,avg}}$ is the gate-open time that follows from a regular pattern of lockages uniformly spaced throughout the day without closing the gates until the next phase starts. The calibration parameter c_{DOT} can be determined by comparison with the irregular pattern of lockages where the gate-open times are known. Where the gate-open times are not known, some means of predicting the lock operation will have to be used.

Figure 3 shows how the salt flux $\dot{M}$ depends on the amount of cycles per day (blue), where the maximum flux occurs at a specific locking frequency. Due to the even spread over 24 hours, a small locking frequency will result in long gate-open times, and long gate-open times result in a fully exchanged lock chamber. This results in the initially linear relationship between locking frequency and salt flux in Figure 3. As the locking frequency increases, the gate-open times reduce, and from the moment that the lock chamber cannot fully exchange, the blue curve will trend downwards. Reducing (only) the locking frequency is therefore not always the most favourable strategy and should instead be combined with a reduction of the gate-open time. Figure 3 also shows the influence of reducing the gate-open times: the red curves show how the salt flux reduces and how the maximum salt flux shifts towards a lower locking frequency as the gate-open time reduces (i.e. as c_{DOT} becomes smaller).

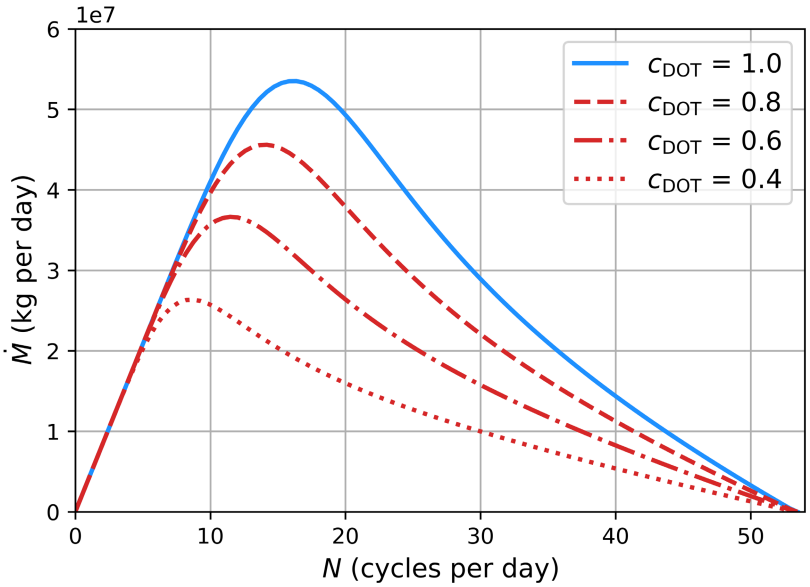

Figure 3: The salt flux (the amount of salt transported per day in kilograms) $\dot{M}$ as a function of the locking frequency (amount of cycles per day) N for different calibration factors c_{DOT}.

Another calibration parameter ($c_{\mathrm{F,Avg}}$) was introduced to describe the lock operation, representing asymmetry by indicating whether the gates on both sides of the lock are open for an equal amount of time ($c_{\mathrm{F,Avg}} = 1$), the gate on the lake side is effectively never open ($c_{\mathrm{F,Avg}} = 0$), or that the gate on the sea side is effectively never open ($c_{\mathrm{F,Avg}} = 2$). This results in the representative gate-open times T_{open} on the fresh and salt side, respectively:

$$T_{\text{open,F}} = C_{\text{F,avg}} T_{\text{open}} \tag{37}$$

$$T_{\text{open,S}} = (2 - C_{\text{F,avg}}) T_{\text{open}} \tag{38}$$

This asymmetry in gate-open times can occur when, at a certain time of day, there is a dominant ship traffic direction as leaving the lock is quicker than entering the lock. A larger degree of asymmetry further reduces the salt flux through the lock, when compared with a situation with the same total number of lockages in a symmetric operation. Both calibration factors, c_{DOT} and $c_{\text{F,avg}}$, depend on the specific characteristic of a lock and its operation.

3 Validation

The individual components of the SLF are based on well-known and extensively studied physical phenomena (see Chapter 1 & 2) and utilize empirical relations from published literature on laboratory studies and prototype field studies in real locks. The added value of the SLF lies in the emphasis on lock operation, and in that it chains all separately validated events and equations together in one continuous locking cycle for the first time. Field measurements have therefore been used to validate the phase-wise SLF. The Quantity of Interest (Oberkampf and Roy, 2013) that was used for validation is the cumulative transport of salt mass over a day of (irregular) locking cycles.

The field measurements took place in the Stevin Lock in the Afsluitdijk, located in between the Wadden Sea and Lake IJssel in the Netherlands, and were performed by Uittenbogaard (2011). These measurements took place in 2010 with the goal of testing the effectiveness of various (combinations of) mitigation measures (Keetels et al., 2011). Table 1 describes the geometry of the Stevin Lock. All remaining boundary conditions and lock operation characteristics vary in time and were captured during the field measurements.

Table 1: Characteristics of the Stevin Lock in the Netherlands.

Category	**Parameter**	**Value**
Geometry	Lock chamber length	148.6 m
	Lock chamber width	14.3 m [(2)]
	Lock chamber floor	−4.7 m DAT
	Sill height lake side	0.30 m
	Sill height sea side	

The field measurements consisted of water level, conductivity, temperature and pressure measurements. The water level measurements were conducted at three locations: inside the lock chamber and in both approach harbours. A total of thirty-five Conductivity Temperature Depth (CTD) sensors were placed at seven (horizontal) locations, one in each approach harbour and five within the lock chamber, with five sensors at each location (vertically) to cover the entire depth at each location. The sensors recorded the conductivity, temperature and pressure every two minutes. The sensors inside the lock chamber were located along the west side – captains were instructed to moor their ships on the east side – at 12.20, 35.75, 65.99, 87.04 and 113.54 m from the gate on the Lake IJssel side. Of the five rows of sensors, the top three were attached to floating buoys, resulting in 0.5, 1.0 and 1.5 m distance between the water surface and the sensors. The bottom two rows of sensors were attached to a stationary frame at 0.5 and 1.5 m from the chamber floor. The vertical lines in the approach harbours were attached to floating buoys located approximately fifty metres from the gates. The water levels in the approach harbours, lock chamber and the atmospheric pressure were measured by separate pressure sensors. The status of the lock gates and levelling valves was tracked throughout the entire period to be able to reconstruct the timing of the different phases in the locking cycles. Characteristics of ships that were present in the lock chamber were retrieved from (anonymized) data in Informatie- en Volgsysteem Scheepvaart (IVS), a ship tracking system that

[(2)] The lock chamber of the Stevin Lock does not have a constant width over its entire depth: the applied width of 14.3 m is the average of a width of 14 m near the water surface and a width of 14.6 m near the bottom.

records information of ships that sail Dutch inland waterways. An example of some of the data that was collected during the field measurements is shown in Figure 4.

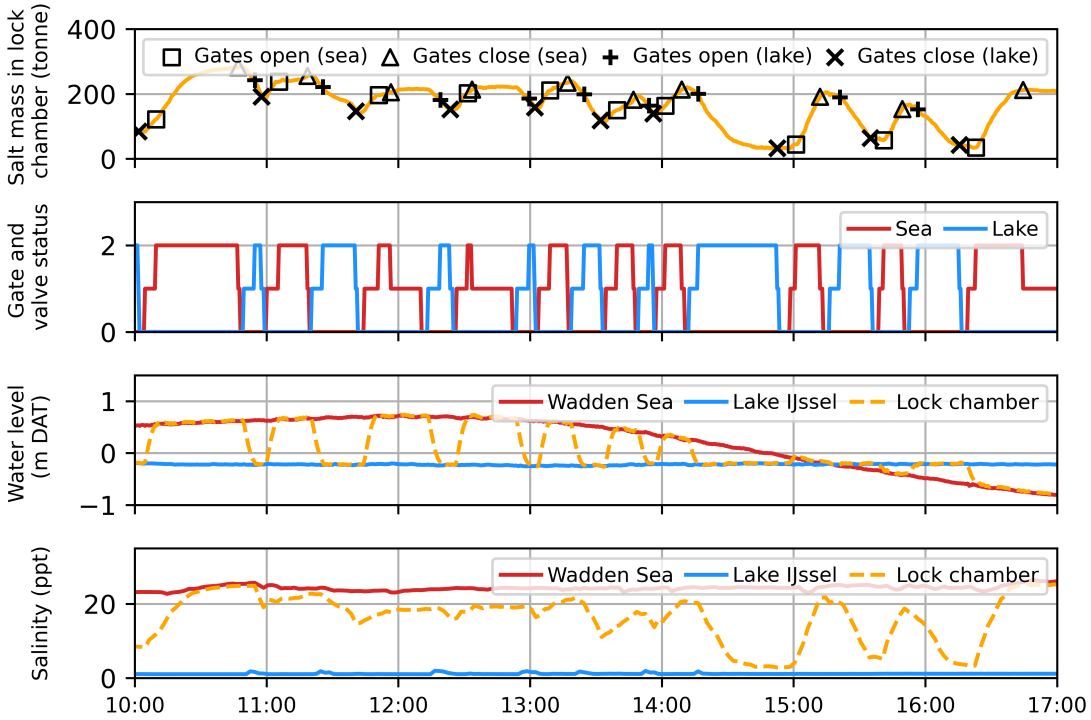

Figure 4: Example of field measurement data that was retrieved on April 2nd, 2010 in the Stevin Lock in the Netherlands. From top to bottom: salt mass in the lock chamber in tonnes, the status of the valves and gates: all closed (0), levelling valves open (1) or lock gates open (2), and the water levels and depth-averaged salinities in the Wadden Sea, Lake IJssel and within the lock chamber.

The salt mass in the lock chamber (top in Figure 4) was determined by integration over partial lock chamber volumes centred around each of the twenty-five CTD sensors in the lock chamber (Uittenbogaard, 2011). The mass of transported salt was calculated by comparing the salt mass in the lock chamber at the start and end of a locking phase as indicated by the status of the gates (second from top in Figure 4). The measured transported salt mass can be compared to the outcome of the phase-wise SLF directly. A comparison between the results of the field measurements and SLF calculations is shown in Figure 5 for three days in April 2010. Each step in Figure 5 corresponds to a phase in the locking cycle, either to transported salt mass due to levelling or due to lock exchange flow. Some of the steps show near perfect accuracy, with the overall end result showing a model underestimation of 7 to 10%. Due to the cumulative nature of this validation parameter it is expected that calculations of longer sequences of lockages (days to weeks as opposed to singular days) would result in greater overall accuracy as over- and underestimations partially cancel each other out over time.

Detailed evaluation of the validation results showed that the calculated salt transport due to lock-exchange contributed most to the overall underestimation. Although the discrepancy with measurements per phase is greatest in levelling phases, these discrepancies do not have a systematic under or overestimation and therefore give a low cumulative discrepancy. In addition, the levelling volume is relatively small (scaling with head difference) in each phase compared to the volume which can be exchanged in a lock-exchange phase (scaling with total lock volume).

Some factors that may contribute to the overall discrepancy are the (in practice) remaining head difference when opening the gates(1), a change of the tides during the levelling phase, and stratification, which may cause an over- or underestimation of the speed of the density current due to the assumption of depth-averaged salt concentrations (Dai, 2017). Most sea locks in the Netherlands, have the property, like the Stevin lock here, that the contribution of the lockage prism to the salt intrusion is much smaller than the contribution of the lock exchange flow. Exceptions to this are locks with head differences that are very large compared to the depth of the lock combined with large ships that block a large part of the cross-sectional area of the lock chamber, or combined with short gate-open times. The contribution of the lockage prism can be greater in that case. Similarly, for ship displacement there can be exceptional cases in which that

plays a larger role than in this validation case. Further research into possible improvements to the SLF is ongoing, including validation of the available mitigation measures (bubble screens, sills and flushing).

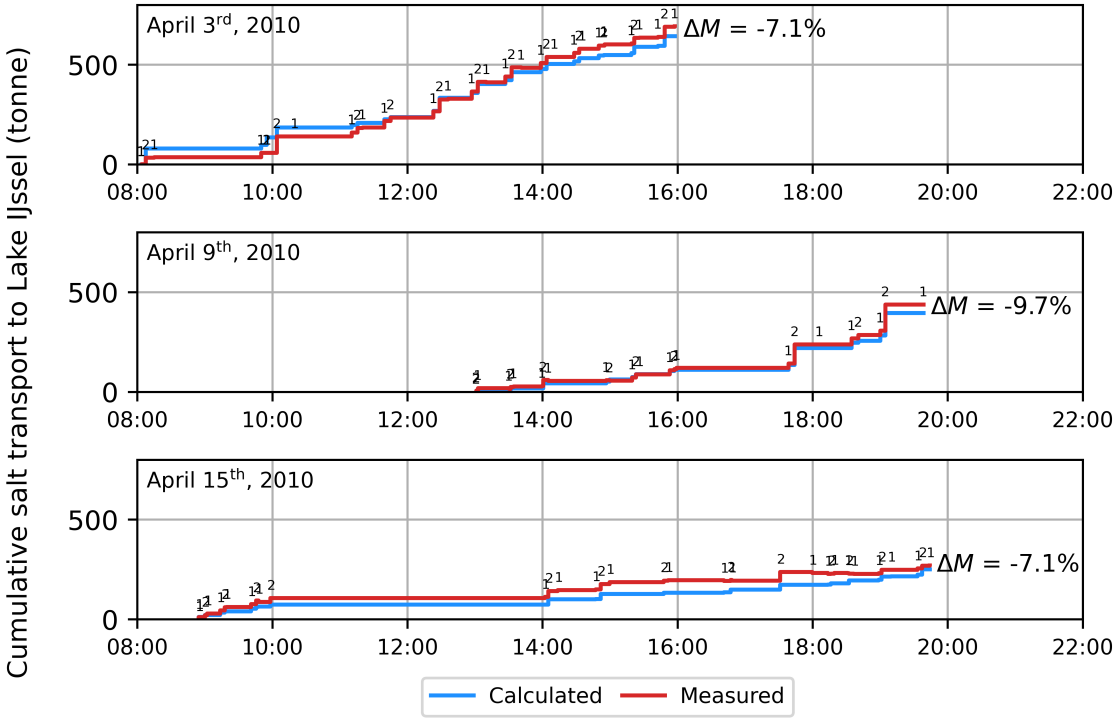

Figure 5: Comparison between field measurements (red) and SLF calculations (blue) of the cumulative transport (indicated per phase) of salt to Lake IJssel through the Stevin Lock on several days in April 2010. Each step in the cumulative transport is marked by the relevant phase of the lockage cycle: 1 (levelling towards the freshwater side) or 2 (lock exchange on the freshwater side).

4 Applications

Generally speaking, the SLF can be used to quantify the functional performance (Van Baaren et al., 2023) of current and future sea locks, in this particular case meaning to quantify how well a sea lock performs its function and fulfils any requirements regarding salt intrusion. Many locks in the Netherlands will require renewal or renovation in the coming years due to aging of the structure itself. Assessing the current functional performance using the SLF can aid in determining at what point in time decisions need to be made on renewing or renovating a sea lock. The SLF is also applicable outside of the Netherlands, for example at the locks in the Lake Washington Ship Canal in Seattle (Mausshardt and Singleton, 1995), Barrage d'Arzal-Camoël in France and Cardiff Bay Barrage in the UK (Burt, 2002; PIANC, 2021) and with small adaptations also to locks in series, such as those in the Panama Canal (Jongeling, 2003; Parchure et al., 2000; Ruijgh et al., 2023). As freshwater becomes scarce due to climate change, coastal freshwater reservoirs might become more common and sea locks might therefore become more prevalent in the future. The SLF can also be used to determine how well different future design choices will perform under different future circumstances (due to policy changes, climate change or economic development) and what the effects of mitigation measures (Van der Kuur, 1985; Keetels et al., 2011; Mausshardt and Singleton, 1995) are, allowing decisionmakers to weigh different design options.

In the following sections we apply the cycle-averaged SLF to a fictive lock (see Table 2) to illustrate the possibilities for its application.

Table 2: Model parameters (geometry, boundary conditions and lock operation) that describe the fictive lock.

Category	Parameter	Value
Geometry	Lock chamber length	200 m
	Lock chamber width	50 m
	Lock chamber floor	−10 m DAT
Boundary conditions	Salt concentration sea side	25 kg/m^3
	Salt concentration lake side	5 kg/m^3
	Water level sea side	0 m DAT
	Water level lake side	0 m DAT
Lock operation	Number of lockage cycles	15 cycles per day
	Time to open gates	210 s
	Levelling time	600 s
	Calibration coefficient[3]	0.5

4.1 Effects of mitigation measures applied at the lock

There are many different ways to reduce the amount of salt intrusion at sea locks. The most efficient and easy to implement approach to reducing salt intrusion is to reduce the amount of lock cycles and/or to reduce the gate-open times. Figure 3 shows the result of these measures: reducing the gate-open times for the same number of lockages reduces the salt flux. This may however interfere with the nautical operation and the nautical safety. For instance, a larger gate-open time may be required because of the possibility of the gate failing to open when a large seagoing ship is approaching, or because of the effect of the lock exchange flows on a manoeuvring ship. When reducing the gate-open times is deemed not possible, a reduction in the number of lockages can reduce salt intrusion. This so-called 'clustering' means more ships per lockage and thus to longer gate-open times. The net effect may or may not lead to reduced salt intrusion as shown by Figure 3. Another added benefit to a 'full' chamber is that any space taken up by ships cannot be taken up by saltwater. Other mitigating measures might require additional structures, such as sills and bubble screens.

Figure 6 shows the impact of mitigating salt intrusion by using a bubble screen at both lock heads, where the vertical current created by rising bubbles reduces the magnitude of the exchange flow. The calculation uses a constant effectiveness parameter $\eta = 0.50$. This does not mean that the reduction in salt intrusion from the bubble screen is 50%, instead, the reduction depends on the gate-open time and number of cycles (see Section 2.2.2 and Equation (7))[4]. This process only delays the exchange flow and salt will eventually intrude if the lock gates are opened long enough (Abraham, 1976; Keetels et al., 2011; O'Mahoney et al., 2024). It is therefore important to apply this mitigation measure in combination with minimal gate-open times. A bubble screen efficiency of η = 0.50 represents the minimum amount of air that is required to create a stable bubble screen. For an ideal (optimally efficient) bubble screen η = 0.25, which requires a lot of air. Values $\eta < 0.25$ are not realistic. In theory this could be achieved with an even larger flow of air, but the mixing induced by the bubble screen becomes so intense that it counteracts the effect of reducing the lock exchange flow.

Sills are often already present in lock heads to support the gates, but can also be considered as a measure to implement in an existing lock. Naturally, implementing a sill is only possible when the ships have a draught that is small relative to the depth of the lock. For the occasional passing of a ship with a greater draught, the sill would have to be lowered, implying the need for a movable sill. Such a movable sill could also be raised only whenever extra 'protection' is required, for example during droughts. Such a sill is present in the Chittenden locks in Seattle (Mausshardt and Singleton, 1995). Figure 6 also shows the influence of placing sills with a height of 2.0 m at both lock heads, which provide a way to block the salty water at the bed of the waterway. The 'effectiveness' of a sill is equal to 80% (Keetels et al., 2011), meaning that (1) the exchange height in the lock head is reduced with 80% of the sill height when calculating the velocity of the

[3] SLF parameter 'calibration coefficient' refers to c_{DOT}, which allows the user to take the irregular distribution of locking cycles throughout the day into account in the cycle-averaged gate-open time (see Equation (36)).
[4] The introduction of η in Equation (7) implies that only the velocity of the density current is changed, and e.g. the salt concentration of the density current is not. In reality, the bubble screen will cause a lot of mixing, which changes the salinities of the lock exchange flow.

lock exchange and (2), for a sill in the lock head at the fresh side, a salty layer with a thickness of 80% of the height of the sill will remain inside the lock chamber, unaffected by the lock exchange flows. The combination of a bubble screen on top of a sill can be used to acquire the same reduction in salt intrusion at lower energy costs due to the decreased amount of air required.

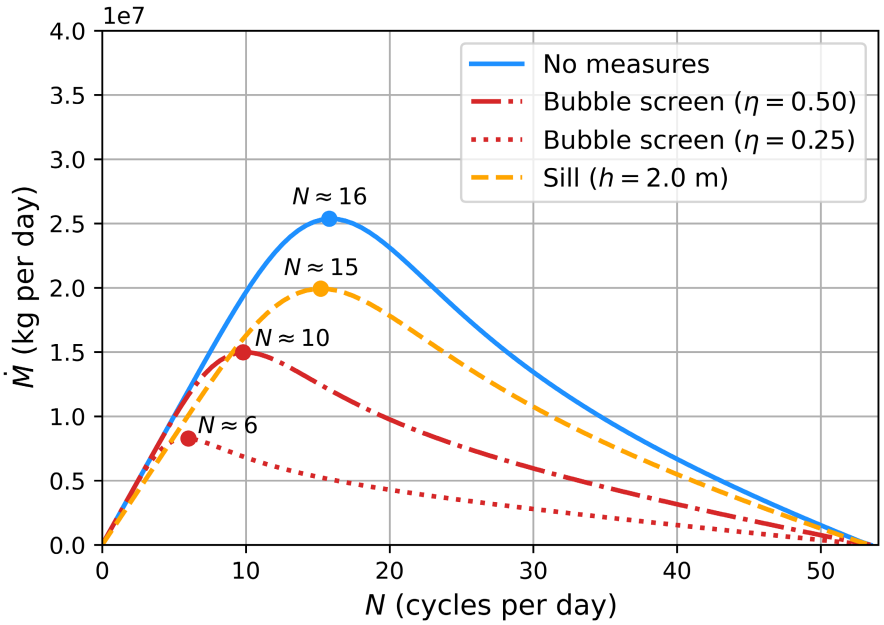

Figure 6: Relationship between locking frequency N and the amount of salt transported per day in kilograms $\dot{M}$ with and without bubble screens or sills at both lock heads. The locking frequency (rounded to the nearest whole number) at which $\dot{M}$ reaches its maximum is indicated per case.

4.2 Effects of sea level rise and lock dimensions

Sea level rise is one of the drivers of salt intrusion (Werner and Simmons, 2009). To quantify the increase in salt intrusion due to sea level rise, we can adjust the water levels at the fictive lock (see Table 2) to include a certain amount of sea level rise at the seaside boundary. An example of assessing the effects of sea level rise on salt transport through the fictive lock is shown in Figure 7. Figure 7 also shows the full bandwidth of the KNMI (2023) 'low' and 'high' scenarios of sea level rise predictions for the Netherlands in 2100. When planning for the future, not only sea level rise should be taken into account. An example of another factor may be economic prosperity: if there is a desire to accommodate more or individually larger ships in the future, any future locks may need to be larger. The consequences of increasing the depth of a lock is also shown in Figure 7. The consequence of increasing the depth is two-fold: in addition to having a greater volume of salt water, the lock-exchange flow will also be faster since the velocity of density currents scales with water depth. The (absolute) additional amount of salt intrusion due to sea level rise is (approximately) equal in each case, but its contribution to the total amount of salt intrusion is relatively small as the lock chamber becomes deeper. This is a result of the extra levelling volume and extra lock-exchange volume, attributable to sea level rise, being relatively small with respect to the total volume of the deeper lock chamber. The length and width of the lock chamber also affect the amount of salt intrusion. Trivially, they both affect the lockage prism and lock chamber volume, while the length also affects the time it takes for the lock chamber to be exchanged fully.

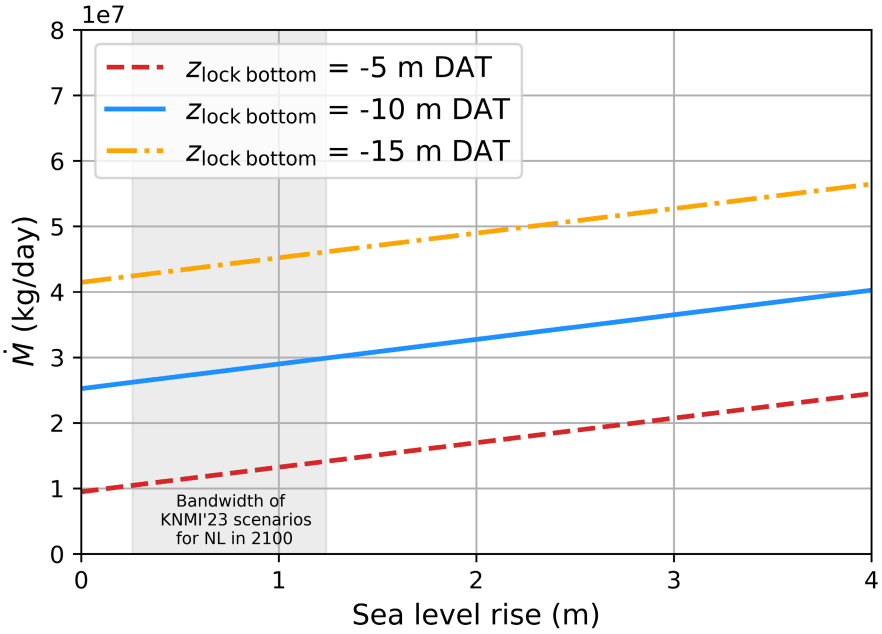

Figure 7: The transported salt per day as a function of sea level rise for the fictive lock (blue solid line, see Table 2) and for similar locks with a smaller (red dashed line) and greater depth (orange dash-dotted line). The full bandwidth of sea level rise predictions for the Netherlands in 2100 is shaded in grey (KNMI, 2023).

4.3 Salt intrusion requirements in the greater water system

Generally speaking, salt intrusion requirements are not imposed as a maximum salt flux through the navigation lock or locks, but rather on the system level, as a certain maximum salt concentration at a location that fulfils a function in the agriculture or drinking water sector. This salt concentration at such a location is not the same as the concentration close to the lock: due to discharge over the canal or lake, the salt concentration at the lock is higher than further upstream. The dispersion of salt over the distance between the two locations has to be considered. The SLF can be used to generate boundary conditions for detailed dispersion modelling using 2DV or 3D Boussinesq models that explicitly model the water system. When the salt concentrations on both sides of the lock are not very sensitive to the effect of the lockages, the flows in and out of the lock can be calculated with the SLF (once) and used as boundary conditions for the salt dispersion model. Whenever the interaction between the lock operation and the local salt concentration is stronger, this interaction should be accommodated in the computational approach (continuous updates).

Another and more simple option is to consider a mass balance over a control volume including the locks and (part of) the fresh water body on the lake or canal side. This mass balance assumes the lock to be accompanied by a sluice gate or pumping station that discharges the superfluous fresh water that comes into the control volume from upstream, possibly together with an incoming levelling discharge, in order to keep the canal or lake level constant. Note that in this mass balance the sign convention is based on whether a discharge flows into (positive) or out of (negative) the control volume and as such differs from the sign convention used in the SLF (see Section 2.1.1).

The influx of salt into the control volume is equal to the incoming discharge from the lock $Q_{\text{lock to lake}}$ and its salt concentration $S_{\text{lock to lake}}$, and to the river discharge Q_{river} with a background salt concentration S_{river}. The outflux is equal to the river discharge with the salt concentration close to the lock S_{F} and to the outgoing discharge through the lock with this same salt concentration S_{F}. For lock exchange, this outgoing discharge is equal to the incoming discharge from the lock but will have different salinities. Levelling discharges are included in the available terms: incoming as part of $Q_{\text{lock to lake}}$ with $S_{\text{lock to lake}}$, which leaves the control volume through the sluice gate together with Q_{river} with S_{F}, and the outgoing levelling discharge (also as part of $Q_{\text{lock to lake}}$) leaves through the lock, again with S_{F}. These terms of the mass balance can be rewritten into a formula which equates a ratio in discharges to a ratio in salt concentration differences:

$$\frac{Q_{\text{river}}}{Q_{\text{lock to lake}}} = \frac{S_{\text{lock to lake}} - S_{\text{F}}}{S_{\text{F}} - S_{\text{river}}} \tag{39}$$

Equation (39) shows that a large river discharge will be required when there is a large (in volume and/or in salt concentration) salt flux coming from the lock or when the salt concentration close to the lock has to stay low, i.e. close to the background salt concentration. In this way, Equation (39) allows quantification of the essence of the water management challenge of limiting salt intrusion through navigation locks.

Using the values from the SLF for the discharge from the lock and its salt concentration, this mass balance allows the investigation of the shift in the equilibrium state of a water system under changing circumstances. An example is shown in Figure 8 for the fictive lock (see Table 2) and a longer and deeper version of the fictive lock. The background salt concentration of the river discharge is equal to 0.2 kg/m^3 in this example. Figure 8 shows that the longer and deeper lock requires almost twice as much river discharge than the fictive lock to keep an equilibrium salt concentration of 2 kg/m^3 on the lake side of the lock. Figure 8 also shows that the increase in the equilibrium salt concentration for a 80 m^3/s reduction in river discharge from 200 m^3/s to 120 m^3/s (in a drought for instance) is much bigger than the increase due to a metre of sea level rise (orange dash-dotted line in Figure 8). A local increase in salt concentration near the lock will also be noticeable at some distance upstream, especially with a reduced river discharge. This indicates that water systems with sea locks may be threatened more seriously by drought than by sea level rise. Note that, as follows from the described mass balance, Figure 8 presents equilibrium states of the water system. The size and structure of the hinterland, with its corresponding (local) variations in salt concentration along its length and depth, are not considered.

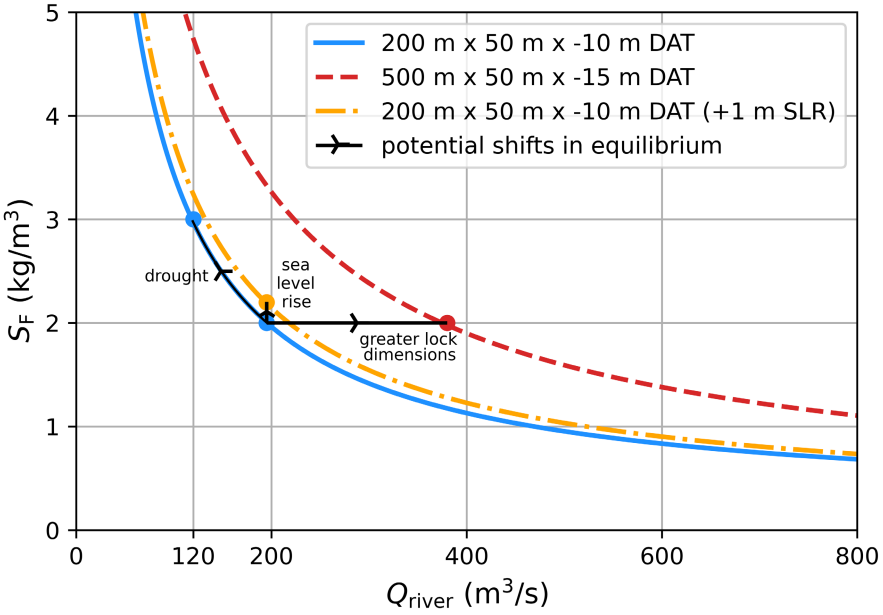

Figure 8: The shift in the equilibrium between freshwater discharge Q_{river} and the salt concentration in the inner approach harbour S_{F} for the fictive lock (blue solid line, see Table 2), a longer and deeper version of the fictive lock (red dashed line), and the fictive lock with one metre of sea level rise (SLR) (orange dash-dotted line).

5 Conclusions

The developed model is compact and allows quick quantification of the influence of salt intrusion through sea locks on upstream freshwater bodies, given changes in lock operation or design, climate change and socioeconomic trends. Mitigation measures can be applied in the form of sills or bubble screens. The empirical relations upon which the model is based have been derived from field scale measurements. Considering that the lockage cycle can be broken up into distinct phases, these relations can be combined in such a way that it is applicable to another lock or lock operation protocol. This makes the SLF applicable in a broad range of situations. Validation using field measurements showed an

underestimation of 7–10% by the model when run per phase. For similar accuracy with the cycle-averaged equations a further calibration is needed.

While the SLF is useful for generating boundary conditions for other models for the dispersion of saltwater intrusion into inland freshwater systems, the model can also be used on its own to determine some relations specific to the locks themselves. Efforts are underway to integrate the SLF into both 3D hydrodynamic models and in decision support systems for operational saltwater management.

Salt intrusion through locks is the consequence of many lockages in sequence. A method which assumes a fully exchanged lock chamber of seawater emptying into the inland system can massively overestimate the salt intrusion. Instead, a sequence of partial lockages ensures that the salt concentration of the lock chamber when the inner gate is opened shows an intermediate value due to the influence of both outer and inner harbour waters. Consequently, reducing the number of lockages may not necessarily reduce the total salt intrusion, if as a result of the increased difficulty in operation of the lock (more ships in each lockage, making manoeuvring difficult) the gate-open times increase. This strategy could therefore be counterproductive in times of drought. However, reducing the gate-open times is a very effective measure to reduce salt intrusion. Still, it is important that the reduction of the gate-open times does not interfere with nautical safety.

Sea level rise affects salt intrusion in two main ways: through the lockage prism, which on the sea side of the lock becomes larger at high tide, and through an increased lock exchange flow on the sea side (the density current has an increased height and an increased speed, owing to the increased water depth). For deeper lock chambers the effect of sea level rise is relatively small as the increase in the lockage prism and increase in the lock-exchange flow is small (in the order of one to two metres of sea level rise) compared to the lock-exchange flow that already occurs in a deep lock (for sea locks in the order of ten to twenty metres of depth). As a consequence of this, inland freshwater systems for which sea locks are the primary or dominant source of salt intrusion, may be threatened more seriously by drought (reduced flushing discharge) than by sea level rise. The SLF is a suitable model to further analyse the impact of these phenomena in combination with their respective probabilities. It also incorporates the many published empirical relations on the effectiveness of mitigation measures.

Acknowledgements

Funding

The authors acknowledge the support and funding by Deltares, Rijkswaterstaat and *Kennisprogramma Natte Kunstwerken* (“Knowledge Programme Hydraulic Structures”).

Author contributions (CRediT)

Weiler, O.M.: Conceptualization, Methodology, Funding acquisition, Supervision, Writing – Review & Editing. Vreeken, T.: Methodology, Software, Data Curation. Maijvis, S.D.: Validation, Visualization, Writing – Original Draft, Writing – Review & Editing. Zuiderwijk, N.L.: Validation, Data Curation, Writing – Review & Editing. O'Mahoney, T.S.D.: Funding acquisition, Supervision, Validation, Writing – Original Draft, Writing – Review & Editing.

Use of AI

No AI was used in the creation of the Sea Lock Formulation or in writing this paper.

Data access statement

The Sea Lock Formulation is open source and is available through GitHub repository *D-SLF*. The full dataset of the Stevin Lock experiments is open access and is available through platform Waterinfo Extra: Praktijkproef Stevinsluis.

Conflict of Interest (COI)

The authors report no conflict of interest.

Notation

Name	Symbol	Unit
Bubble screen effectivity (reduction factor)	η	-
Density	ρ	kg/m^3
The average water density across both sides of the lock head	$\bar{\rho}$	kg/m^3
Calibration parameter for daily gate-open time distribution	c_{DOT}	-
Calibration parameter for gate-open time symmetry between lock heads	$c_{\mathrm{F,Avg}}$	-
Density current velocity	c_i	m/s
Gravitational acceleration	g	m/s²
Water depth	H	m
Water depth at the fresh lock head	H_{F}	m
Water depth at the salt lock head	H_{S}	m
Water level on the freshwater side	h_{F}	m DAT
Water level in the lock chamber	h_{L}	m DAT
Water level on the saltwater side	h_{S}	m DAT
Length of the lock chamber	L_{L}	m
Transported salt mass	M	kg
Average transported salt mass	$\bar{M}$	kg
Salt flux	$\dot{M}$	kg/s
Transported salt mass over the lock head on the freshwater side	M_{F}	kg
Cycle-averaged mass flux to the freshwater side	$\dot{M}_{\mathrm{F}}$	kg/s
Total salt mass transported to the freshwater side in phase 1	$M_{\mathrm{F,1}}$	kg
Total salt mass transported to the freshwater side in phase 2	$M_{\mathrm{F,2}}$	kg
Salt mass transported to the freshwater side by ships exiting the lock in phase 2	$M_{\mathrm{F,2a}}$	kg
Salt mass transported to the freshwater side by lock exchange flow in phase 2	$M_{\mathrm{F,2b,LE}}$	kg
Salt mass transported to the freshwater side by ships entering the lock in phase 2	$M_{\mathrm{F,2c}}$	kg
Salt mass transport due to levelling at low tide	$M_{\mathrm{F,LT1}}$	kg
Salt mass transport due to levelling at high tide	$M_{\mathrm{F,HT1}}$	kg
Transported salt mass over the lock head on the saltwater side	M_{S}	kg
Cycle-averaged mass flux to the saltwater side	$\dot{M}_{\mathrm{S}}$	kg/s
Total salt mass transported to the saltwater side in phase 3	$M_{\mathrm{S,3}}$	kg
Total salt mass transported to the saltwater side in phase 4	$M_{\mathrm{S,4}}$	kg
Salt mass transported to the freshwater side by ships exiting the lock in phase 4	$M_{\mathrm{S,4a}}$	kg
Salt mass transported to the freshwater side by lock exchange flow in phase 4	$M_{\mathrm{S,4b,LE}}$	kg
Salt mass transported to the freshwater side by ships entering the lock in phase 4	$M_{\mathrm{S,4c}}$	kg
Discharge	Q	m³/s
Discharge from the lock chamber to the freshwater side	$Q_{\mathrm{lock\ to\ lake}}$	m^3/s
Discharge from the freshwater side to the lock chamber	$Q_{\mathrm{lake\ to\ lock}}$	m^3/s

Name	Symbol	Unit
River discharge	Q_{river}	m³/s
Salt concentration of the freshwater side	S_{F}	kg/m³
Salt concentration of the discharge from the lock chamber to the freshwater side	$S_{\text{lock to lake}}$	kg/m³
Salt concentration of the lock after phase 3	$S_{\text{L,F,Lev}}$	kg/m³
Salt concentration of the lock after phase 2	$S_{\text{L,2}}$	kg/m³
Salt concentration of the lock after ships exiting the lock in phase 2	$S_{\text{L,2a}}$	kg/m³
Salt concentration of the lock after lock exchange in phase 2	$S_{\text{L,2b}}$	kg/m³
Salt concentration of the lock after phase 4	$S_{\text{L,4}}$	kg/m³
Salt concentration of the lock after ships exiting the lock in phase 4	$S_{\text{L,4a}}$	kg/m³
Salt concentration of the lock after lock exchange in phase 4	$S_{\text{L,4b}}$	kg/m³
Salt concentration of the lock after lock exchange flow with the saltwater side	$S_{\text{L,S}}$	kg/m³
Salt concentration of the lock after phase 1	$S_{\text{L,S,Lev}}$	kg/m³
Salt concentration of the saltwater side	S_{S}	kg/m³
Background salt concentration	S_{river}	kg/m³
Time for a density current to travel the length of a lock chamber twice	T_{LE}	s
Representative gate-open time	T_{open}	s
Average gate-open time	$T_{\text{open,avg}}$	s
Representative gate-open time on the freshwater side	$T_{\text{open,F}}$	s
Representative gate-open time on the saltwater side	$T_{\text{open,S}}$	s
Average time for a complete locking cycle	T_{cycle}	s
Volume	V	m³
Lock chamber volume	V_{L}	m³
Volume moved between lock and approach harbour due to levelling at low tide	$V_{\text{Lev,LT}}$	m³
Volume moved between lock and approach harbour due to levelling at high tide	$V_{\text{Lev,HT}}$	m³
Lock chamber volume when levelled with the freshwater side	$V_{\text{L,F}}$	m³
Lock chamber volume when levelled with the saltwater side	$V_{\text{L,S}}$	m³
Volume discharged from the lock towards the freshwater side	$V_{\text{lock to lake}}$	m³
Volume discharged from the freshwater side towards the lock	$V_{\text{lake to lock}}$	m³
Total water displacement by ships moving upstream	$V_{\text{Ship,Up}}$	m³
Total water displacement by ships moving downstream	$V_{\text{Ship,Down}}$	m³
Volume moved between lock and approach harbour due to lock exchange flow	V_{U}	m³
Volume moved between lock and freshwater side due to lock exchange flow	$V_{\text{U,F}}$	m³
Volume moved between lock and saltwater side due to lock exchange flow	$V_{\text{U,S}}$	m³
Width of the lock chamber	W_{L}	m
Depth of the lock chamber floor	z_{L}	m DAT
Dimensionless salt transport per cycle	Z_{fraction}	-

References

Abraham, G. (1976). Density currents due to differences in salinity. *Proceedings of a seminar on Salt distribution in Estuaries* (pp. 11-40). The Hague: Government Publishing Office, ISBN 9012012953.

Abraham, G., and van den Burgh, P. (1964). Pneumatic Reduction of Salt Intrusion through Locks. *Journal of the Hydraulics Division, ASCE, 90*(1), 83-119. https://doi.org/10.1061/JYCEAJ.0001009

Akter, R., Asik, T. Z., Sakib, M., Akter, M., Sakib, M. N., Al Azad, A. S., Maruf, M., Haque, A., and Rahman, M. M. (2019). The Dominant Climate Change Event for Salinity Intrusion in the GBM Delta. *Climate, 7*(69). https://doi.org/10.3390/cli7050069

Augustijn, D. C., van den Berg, M., de Bruine, E., and Korving, H. (2011). Dynamic Control of Salt Intrusion in the Mark-Vliet River System, The Netherlands. *Water Reources Management, 25*, 1005-1020. https://doi.org/10.1007/s11269-010-9738-1

Bain, R. L., Hale, R. P., and Goodbred, S. L. (2019). Flow Reorganization in an Anthropogenically Modified Tidal Channel Network: An Example From the Southwestern Ganges-Brahmaputra-Meghna Delta. *Journal of Geophysical Research: Earth Surface, 124*(8), 2141-2159. https://doi.org/10.1029/2018JF004996

Bricheno, L. M., Wolf, J., and Sun, Y. (2021). Saline intrusion in the Ganges-Brahmaputra-Meghna megadelta. *Estuarine, Coastal and Shelf Science, 252*, 107246. https://doi.org/10.1016/j.ecss.2021.107246

Brooke Benjamin, T. (1968). Gravity currents and related phenomena. *Journal of Fluid Mechanics, 31*(2), 209-248. https://doi.org/10.1017/S0022112068000133

Burt, N. (2002). Cardiff Bay Barrage: overview of hydraulic studies. *Proceedings of the Institution of Civil Engineers - Water and Maritime Engineering, 154*(2), 93-102. https://doi.org/10.1680/wama.154.2.93.38668

Chen, W., Chen, K., Kuang, C., Zhu, D. Z., He, L., Mao, X., Liang, H., and & Song, H. (2016). Influence of sea level rise on saline water intrusion in the Yangtze River Estuary. *China Applied Ocean Research, 54*, 12- 25. https://doi.org/10.1016/j.apor.2015.11.002

Costall, A. R., Harris, B. D., Teo, B., Schaa, R., Wagner, F. M., and Pigois, J. P. (2020). Groundwater Throughflow and Seawater Intrusion in High Quality Coastal Aquifers. *Nature Scientific Reports, 10*. https://doi.org/10.1038/s41598-020-66516-6

Cuthbertson, A., Laanearu, J., Carr, M., Sommeria, J., and Viboud, S. (2018). Blockage of saline intrusions in restricted, two-layer exchange flows across a submerged sill obstruction. *Environmental Fluid Mechanics, 18*, 27-57. https://doi.org/10.1007/s10652-017-9523-2

Dai, A. (2017). Experiments on two-layer density-stratified inertial gravity currents. *Physical Review Fluids, 2*. https://doi.org/10.1103/PhysRevFluids.2.073802

De Goede, E. D. (2020). Historical overview of 2D and 3D hydrodynamic modelling software of shallow water flows in the Netherlands. *Ocean Dynamics, 70*, 521-539. https://doi.org/10.1007/s10236-019-01336-5

De Groot, I. (2015). *WANDA-Locks, het nieuwe zoutlekmodel.* Delft, the Netherlands: Deltares, Reference: 1209463-000-HYE-0002 (technical report, in Dutch).

Ekin Aydin, B., Tian, X., Delsman, J., Oude Essink, G. H., and Rutten, M. (2019). Optimal salinity and water level control of water course using Model Predictive Control. *Environmental Modelling and Software, 112*, 36-45. https://doi.org/10.1016/j.envsoft.2018.11.010

El-Agha, D. E., Molle, F., Rap, E., El Bialy, M., and El-Hassan, W. A. (2020). Drainage water salinity and quality across nested scales in the Nile Delta of Egypt. *Environmental Science and Pollution Research, 27*, 32239-32250. https://doi.org/10.1007/s11356-019-07154-y

Ferguson, G., and Gleeson, T. (2012). Vulnerability of coastal aquifers to groundwater use and climate change. *Nature Climate Change, 2*(5), 342-345. https://doi.org/10.1038/nclimate1413

Galván, C., Puente, A., Castanedo, S., and Juanes, J. (2016). Average vs. extreme salinity conditions: Do they equally affect the distribution of macroinvertebrates in estuarine environments? *Limnology and Oceanography, 61*, 984-1000. https://doi.org/10.1002/lno.10267

Genseberger, M., and Bijlsma, A. C. (2016). *Actualisatie 3D zoutverspreidingsmodel IJsselmeer.* Delft, the Netherlands: Deltares, Reference: 1230069-000-ZKS-0033 (technical report, in Dutch).

Genseberger, M., Fujisaki, A., Thiange, C., Eijsberg-Bak, C., Bijlsma, A., and Boderie, P. (2021). Domain Decomposition in Shallow Water Modelling of Dutch Lakes for Multiple Applications. *26th International Conference on Domain Decomposition Methods in Science and Engineering (2020)*, (pp. 281-289). Hong Kong. https://doi.org/10.1007/978-3-030-95025-5_29

Gong, W., Shen, J., and Jia, L. (2013). Salt intrusion during the dry season in the Huangmaohai Estuary, Pearl River Delta, China. *Journal of Marine Systems, 111-112*, 235-252. https://doi.org/10.1016/j.jmarsys.2012.11.006

Haasnoot, M., Kwadijk, J., van Alphen, J., Le Bars, D., van den Hurk, B., Diermanse, F., van der Spek, A., Oude Essink, G., Delsman, J., and Mens, M. (2020). Adaptation to uncrtain sea-level rise; how uncertainty in Antartic mass-loss impacts the coastal adaptation strategy of the Netherlands. *Environmental Research Letters, 15*. https://doi.org/10.1088/1748-9326/ab666c

Hagen, S. C., and Irish, J. L. (2013). Implications, Planning, and Design Coniderations for Rising Sea Levels at the Coast. *Journal of Waterway, Port, Coastal and Ocean Engineering, 139*(2). https://doi.org/10.1061/(ASCE)WW.1943-5460.0000186

Hagen, S. C., Morris, J. T., Bacopoulos, P., and Wesihampel, J. F. (2013). Sea-Level Rise Impact on a Salt March System of the Lower St. Johns River. *Journal of Waterway, Port, Coastal and Ocean Engineering, 139*(2), 118-125. https://doi.org/10.1061/(ASCE)WW.1943-5460.0000177

Hendriks, D. M., Kuijper, M. J., and van Ek, R. (2014). Groundwater impact on environmental flow needs of stream in sandy catchments in the Netherlands. *Hydrological Sciences Journal, 59*(3-4), 562-577. https://doi.org/10.1080/02626667.2014.892601

Huizer, S., Karaoulis, M. C., Oude Essink, G. H., and Bierkens, M. F. (2017). Monitoring and simulation of salinity changes in response to tide and strom surges in a sandy coastal aquifer system. *Water Resources Research, 53*. https://doi.org/10.1002/2016WR020339

IPCC. (2014). Climate Change 2014: Impacts, Adaptation, and Vulnerability. Part A: Global and Sectoral Aspects. Contribution of Working Group II to the Fifth Assessment Report of the Intergovernmental Panel on Climate Change. In *Fifth Assessment Report IPCC.* Cambridge, United Kingdom and New York, NY, USA: Cambridge University Press. https://doi.org/10.1017/CBO9781107415379

Jongeling, T. (2003). *Salt water intrusion analysis Panama canal Locks. Existing situation. Report A: Field data collection, development and validation of simulation model, analysis of salt water intrusion Q3039.* Delft, the Netherlands: WL | Delft Hydraulics.

Keetels, G., Uittenbogaard, R., Cornelisse, J., Villars, N., and van Pagee, H. (2011). Field Study and Supporting Analysis of Air Curtains and Other Measures to Reduce Salinity Transport through Shipping Locks. *Irrigation and Drainage, 60*(1), 42-50. https://doi.org/10.1002/ird.679

Kerstma, J., Kolkman, P. A., Regeling, H. J., and Venis, W. A. (1994). *Water Quality Control at Ship Locks.* Rotterdam, the Netherlands: A. A. Balkeman, ISBN 9054101423.

KNMI. (2023). *KNMI'23 Klimaatscenario's voor Nederland (gebruikersrapport) (in Dutch).* De Bilt, the Netherlands: KNMI.

Lowe, J. A., Howard, T. P., Pardaens, A., Tinker, J., Holt, J., Wakelin, S., Milne, G., Leake, J., Wolf, J., Horsburgh, K., Reeder, T., Jenkins, G., Ridley, J., Dye, S., and Bradley, S. (2009). *UK Climate Projections science report: Marine and coastal projections.* Exeter, UK: Met Office Hadley Centre.

MacCready, P., and Geyer, W. R. (2010). Advances in Estuarine Physics. *Annual Review of Marine Science, 2*, 35-58. https://doi.org/10.1146/annurev-marine-120308-081015

Martens, C., Liek, G., Maes, D., Haas, H., Deschamps, M., Dekker, L., van 't Westeinde, H., Vereirssen, M., Verbeek, H., and Storm, K. (2018). Building a Decision Support System of the Terneuzen Locks: Combining Optimal Management for Water and Shipping. *34th PIANC World Congress 2018 in Panama City, Panama: abstracts*, (pp. 244-246). Panama City, Panama.

Martyr-Koller, R. C., Kernkamp, H., van Dam, A., van der Wegen, M., Lucas, L. V., Knowles, N., Jaffe, B., and Fregoso, T. A. (2017). Applicaton of an unstructured 3D finite volume numerical model to flows and salinity dynamics in the San Francisco Bay-Delta. *Estuarine, Coastal and Shelf Science, 192*, 86-107. https://doi.org/10.1016/j.ecss.2017.04.024

Mausshardt, S., and Singleton, G. (1995). Mitigating Salt-Water Intrusion through Hiram M. Chittenden Locks. *Journal of Waterway, Port, Coastal and Ocean Engineering, 121*(4), 224-227. https://doi.org/10.1061/(ASCE)0733-950X(1995)121:4(224)

McAnally, W., and Pritchard, D. W. (1997). Salinity Control in Mississippi River under Drought Flows. *Journal of Waterway, Port, Coastal and Ocean Engineering, 123*(1), 34-40. https://doi.org/10.1061/(ASCE)0733-950X(1997)123:1(34)

Mosley, L. M. (2015). Drought impacts on the water quality of freshwater systems; review and integration. *Earth-Science Reviews, 140*, 203-214. https://doi.org/10.1016/j.earscirev.2014.11.010

Nguyen, A. D., and Savenije, H. H. (2006). Salt intrusion in multi-channel estuaries: a case study in the Meking Delta, Vietnam. *Hydrology and Earth System Sciences, 10*, 743-754. https://doi.org/10.5194/hess-10-743-2006

Nogueira, H. I., van der Ven, P., O'Mahoney, T., de loor, A., van der Hout, A., and Kortlever, W. (2018). Effect of Density Difference on the Forces Acting on a Moored Vessel While Operating Navigation Locks. *Journal of Hydraulic Engineering, 144*(6). https://doi.org/10.1061/(ASCE)HY.1943-7900.0001445

Nogueira, H., Van der Hout, A., O'Mahoney, T., and Kortlever, W. (2023). The Impact of Density Differences on the Hydraulic Design of Leveling Systems: The Case of New Large Sea Locks in IJmuiden and Terneuzen. *Journal of Waterway, Port, Coastal, and Ocean Engineering, 150*(1). https://doi.org/10.1061/JWPED5.WWENG-1993

Oberkampf, W. L., and Roy, C. J. (2013). *Verification and Validation in Scientific Computing.* Cambridge, England: Cambridge University Press. https://doi.org/10.1017/CBO9780511760396

O'Mahoney, T. S., Oldenziel, G., and Van der Ven, P. (2024). The Effect of Bubble Size on Lock-Exchange Density Currents through Bubble Screens. *Journal of Hydraulic Engineering, 150*(3). https://doi.org/10.1061/JHEND8.HYENG-13531

Oude Essink, G. H., van Baaren, E. S., and de Louw, P. G. (2010). Effects of climate change on coastal groundwater systems; A modelling study in the Netherlands. *Water Resrouces Research, 46*. https://doi.org/10.1029/2009WR008719

Parchure, T. M., Wilhelms, S. C., Sarruff, S., and McAnally, W. H. (2000). *Salinity Intrusion in the Panama Canal - ERDC/CHL TR-00-4.* Vicksburg, MS: Coastal and Hydraulics Laboratory, US Army Engineer Research and Development Center. https://doi.org/10.21236/ada378475

PIANC. (2021). *Saltwater Intrusion Mitigation in Inland Waterways.* PIANC InCom WG 198.

Prasad, K. V., Sridevi, T., and Sadhuram, Y. (2018). Influence of Dam-Controlled River Discharge and Tides on Salinity Intrusion in the Godavari Estuary, East Coast of India. *Journal of Waterway, Port, Coastal en Ocean Engineering, 144*(2). https://doi.org/10.1061/(ASCE)WW.1943-5460.0000430

Prinsen, G., Sperna Weiland, F., and Ruijgh, E. (2015). The Delta Model for Fresh Water Policy Analysis in the Netherlands. *Water Resource Management, 29*, 645-661. https://doi.org/10.1007/s11269-014-0880-z

Ralston, D. K., and Geyer, W. R. (2019). Response to channel deepening of the salinity intrusion, estuarine circulation, and stratification in an urbanized estuary. *Journal of Geophysical Research: Oceans, 124*(7), 4784-4802. https://doi.org/10.1029/2019JC015006

Rinehimer, J. P., Walton, R., Brettmann, K. L., and Easthouse, K. B. (2019). Mitigating the Intrusion: Modelling the Effects of Lock Operations on the Water Quality in the Lake Washington Ship Canal. *ASCE World Environmental and Water Resources Congress 2019.* Pittsburgh, Pennsylvania. https://doi.org/10.1061/9780784482353.031

Robins, P. E., Skov, M. W., Lewis, M. J., Gimenez, L., Davies, A. G., Malham, S. K., Neill, S. P., McDonald, J. E., Whitton, T. A., Jackson, S. E., and Jago, C. F. (2016). Impact of climate change on UK estuaries: A review of past trends and potential projections. *Estuarine, Coastal and Shelf Science, 169*, 119-135. https://doi.org/10.1016/j.ecss.2015.12.016

Ruijgh, E., Zijl, F., Monroy, J., Dominguez, I., and O'Mahoney, T. (2023). The Lake Gatun Water Quality Model for the Panama Canal. *Proceedings of the 40th IAHR World Congress (Vienna, 2023)*. https://doi.org/10.3850/978-90-833476-1-5_iahr40wc-p1634-cd

Savenije, H. H. (2012). *Salinity and Tides in Alluvial Estuaries, 2nd completely revised edition: salinityandtides.com.* https://doi.org/10.1016/B978-0-444-52107-1.X5000-X

Shin, J. O., Dalziel, S. B., and Linden, P. F. (2004). Gravity currents produced by lock exchange. *Journal of Fluid Mechanics, 521*, 1-34. https://doi.org/10.1017/S002211200400165X

Uittenbogaard, R. E. (2010). *Voorstudie: Ontwerpstudie en Praktijkproef Zoutlekbeperking Volkeraksluizen, Model voor Zoutvrachtberekeningen.* Delft, the Netherlands: Deltares, Reference: 1201226-011 (technical report, in Dutch).

Uittenbogaard, R. E. (2011). *Ontwerpstudie en Praktijkproef Zoutlekbeperking Volkeraksluizen - Beschrijving en resultaten praktijkproef Stevinsluis en evaluatie maatregelen Stevinsluis.* Delft, the Netherlands: Deltares, Reference: 1201226-005-ZKS-0007 (technical report, in Dutch).

Uittenbogaard, R. E., Cornelisse, J., and O'Hara, K. (2015). Water – Air Bubble Screens Reducing Salt Intrusion Through Shipping Locks. *E-proceedings of the 36th IAHR World Congress. 28 June - 3 July 2015, The Hague, the Netherlands*.

UNESCO. (1981). *The practical salinity scale 1978 and the international equation of state of seawater 1980.* . Sidney, B.C., Canada. : Tenth report of the Joint Panel on Oceanographic Tables and Standards (JPOTS), UNESCO technical papers in marine science, No. 36.

Van Baaren, E. S., Breedeveld, J., ten Harmsen van der Beek, N. J., O'Mahoney, T. S., Kramer, N., Berger, H., and Barneveld, A. (2023). Framework functional performance hydraulic structures. *Eighth International Symposium on Life-Cycle Civil Engineering, Milan, Italy, July 2-6, 2023*, 2605-2611. https://doi.org/10.1201/9781003323020-317

Van Beek, A. (2021). *The influence of a flushing discharge on lock-exchange.* MSc. Thesis, Eindhoven University of Technology.

Van den Brink, M., Huismans, Y., Blaas, M., and Zwolsman, G. (2019). Climate Change Induced Salinization of Drinking Water Inlets along a Tidal Branch of the Rhine River: Impact Assessment and an Adaptive Strategy for Water Resources Management. *climate, 7*(49). https://doi.org/10.3390/cli7040049

Van der Kuur, P. (1985). Locks with Devices to Reduce Salt Intrusion. *Journal of Waterway, Port, Coastal and Ocean Engineering, 111*(6), 1009-1021. https://doi.org/10.1061/(ASCE)0733-950X(1985)111:6(1009)

Van der Ven, P. P., O'Mahoney, T. S., and Weiler, O. M. (2018). Methods to Assess Bubble Screens Applied to Mitigate Salt Intrusion Through Locks. *PIANC World Congress Panama City, Panama 2018*.

Van der Ven, P., De Groot, I., Vreeken, D., and Weiler, O. (2015). Simulating Lock Operations in the Generic Salt Intrusion Model WANDA-Locks (Paper 137). *Smart Rivers, Buenos Aires, Argentina, 7-11 September 2015*.

van Rijn, L., Grasmeijer, B., and Perk, L. (2018). Effect of channel deepening on tidal flow and sediment transport: part I—sandy channels. *Ocean Dynamics, 68*, 1457-1479. https://doi.org/10.1007/s10236-018-1204-2

Vu, D. T., Yamada, T., and Ishidaira, H. (2018). Assessing the impact ofsea level rise due to climate change on seawater intrusion in Mekong Delta, Vietnam. *Water Science & Technology, 77*(6), 1632-1639. https://doi.org/10.2166/wst.2018.038

Wang, D. P. (1983). Two-Dimensional Branching Salt Intrusion Model. *Journal of Waterway, Port, Coastal and Ocean Engineering, 109*(1), 103-112. https://doi.org/10.1061/(ASCE)0733-950X(1983)109:1(103)

Wang, H., Li, C., Hu, Y., Zheng, J., and Chen, H. (2024). Analysis of the Saltwater Intrusion Prevention Effect of Pump for Ship Locks in the Estuary. *Lecture Notes in Civil Engineering - Hydraulic Structure and Hydrodynamics, 608*, 133–144. https://doi.org/10.1007/978-981-97-7251-3_12

Weiler, O., Van de Kerk, A. J., and Meeuse, K. J. (2015). Preventing Salt Intrusion Through Shipping Locks: Recent Innovations and Results from a Pilot Setup. *E-proceedings of the 36th IAHR World Congress, 28 June - 3 July 2015* (pp. 233-242). The Hague, the Netherlands: IAHR.

Werner, A. D., and Simmons, C. (2009). Impact of Sea-Level Rise on Sea Water Intrusion in Coastal Aquifers. *Ground Water, 47*(2), 197-204. https://doi.org/10.1111/j.1745-6584.2008.00535.x

Werner, A. D., Ward, J. D., Morgan, L. K., Simmons, C. T., Robinson, N. I., and Teubner, M. D. (2012). Vulnerability indicators of sea water intrusion. *Ground Water, 50*(1), 48-58. https://doi.org/10.1111/j.1745-6584.2011.00817.x